Coherent Tracking of Globalstar Signals Using Partially-Known Spreading Codes

Orlando Peña[1], Gonzalo Seco-Granados[2], José A. López-Salcedo[2]
[1]External consultant, [2]Universitat Autònoma de Barcelona (UAB), IEEC-CERES, Barcelona, Spain

***Abstract*—It is nowadays widely accepted that the future of satellite-based positioning will comprise the combination of conventional Global Navigation Satellite Systems (GNSS) with new Low-Earth Orbit (LEO) satellites specifically designed for positioning, navigation and timing (PNT). In the meantime, opportunistic positioning using existing LEO constellations has become a practical way to showcase the benefits of incorporating LEO satellites in the PNT domain. Among these constellations, Globalstar is particularly interesting because it shares the same spread-spectrum modulation principle as most GNSS. Therefore, Globalstar signals could easily be processed by GNSS receivers with some minor modifications. Unfortunately, the spreading codes for Globalstar are not publicly available, thus preventing the optimal receiver implementation. While some attempts have been done to estimate such codes, or to get rid of them, the present paper shows that tracking of Globalstar signals is possible using a set of, presumably, very similar spreading code sequences to the ones actually used by Globalstar satellites. Experimental results with live recorded signals are provided to confirm this statement.**

***Index Terms*—Satellite navigation, LEO-PNT, Globalstar, Spreading code**

I. Introduction

Low Earth Orbit (LEO) satellite constellations are receiving an increasing interest driven by the advent of the New Space Economy, a global trend that is being pushed by space agencies worldwide to stimulate the development of new technologies and applications that make use of small, low-cost and easy-to-deploy satellites. This trend has been favored by the dramatic cost reduction in the launch and deployment of satellites, which has sparked the interest of many private companies to deploy their own LEO constellation composed of thousands of small or so-called nanosatellites. Existing LEO satellites can be classified into three main applications: the first one is dealing with broadband Internet access with companies such as Iridium, Globalstar or Starlink, the latter deploying thousands of small satellites; the second one is dealing with Earth observation and telemetry, such as some of the satellites of European Copernicus program; and finally the third one is targeting IoT applications such as asset tracking worldwide. IoT is actually the target application where LEO constellations are experiencing the most rapid growth, pushed by companies such as Orbcomm, Kineis, Amazon, and small startups such as Totum and Xona.

This work was supported in part by the Spanish Agency of Research (AEI) under the Research and Development projects PDC2023-145858-I00/AEI/10.13039/501100011033/FEDER-UE, PID2023-152820OB-I00/AEI/10.13039/501100011033/FEDER-UE, as well as by IEEC and the Catalan Government under the New Space Strategy of Catalonia.

979-8-3503-5685-4/24/$31.00 ©2024 IEEE

LEO satellites have recently been acknowledged to be of great interest for positioning applications because they solve many of the limiting problems of Global Navigation Satellite System (GNSS) satellites. First of all, LEO satellites are much closer to the Earth than GNSS satellites, and therefore LEO signals arrive at the user's terminal with a much higher signal strength compared to GNSS signals. This makes possible the reception of LEO signals indoors, and thus facilitates the implementation of indoor positioning with satellite signals. Furthermore, because of the high received power, the signal is less vulnerable to interference, jamming and spoofing, and shorter pieces of signal suffice to provide the same energy per position fix as with GNSS signals, thus reducing the energy consumption and increasing the battery lifetime. The second advantage is that LEO constellations, particularly the ones being planned for the near future, are composed of hundreds or even thousands of satellites, which provide an excellent coverage and geometry even in the worst working scenarios such as deep urban canyons. The third advantage is that LEO satellites move at a much higher speed than GNSS satellites and this facilitates the implementation of Doppler-based positioning with LEO signals [Kas19]. While Doppler observables are known to provide poor accuracy when used standalone, they can help in situations where GNSS signals are blocked by surrounding obstacles [Rie16] or in snapshot GNSS receivers where an initial reference for the user's position is needed to initialize the coarse-time PVT algorithm. Furthermore, and most importantly, the use of Doppler observables is the only alternative for using most of the existing LEO satellites for opportunistic positioning [1], [2]. That is, positioning using signals and systems not originally designed for that purpose.

Opportunistic positioning using LEO satellites has received an increasing interest in the recent years as first and straigtforward way to complement GNSS without deploying additional satellites. It is thus the natural step before truly dedicated LEO-PNT satellites are available, and it often serves as a benchmark to showcase most of the advantages that future LEO-PNT satellites will bring.

Among the existing LEO satellites, Globalstar ones are particularly interesting because they broadcast signals using the same spread-spectrum modulation principle as most GNSS signals. In this way, Globalstar signals could eventually be processed by GNSS receivers with relatively minor modifications. The problem is that spreading codes used by Globalstar satellites are not explicitly available in the existing literature, thus hindering the processing of Globalstar signals by the general public. Some attempts have been pursued to circumvent this limitation. For instance, a brute-force approach is proposed in [3] to estimate the Globalstar spreading codes

and thus being able to track any LEO satellite in a blind manner. Alternatively, the work in [4] intends to remove the spreading code by raising the received signal to the fourth-power, and thus removing the QPSK signaling induced by the two binary spreading codes present at the in-phase and quadrature component of Globalstar signals. In contrast to these existing works, the present paper unveils some details on how the Globalstar spreading codes are presumably generated, and presents results validating such statement.

The paper is organized as follows.

II. Globalstar Constellation and Signals

A. Overview of the Globalstar constellation

The Globalstar first-generation constellation was composed of 48 satellites orbiting at 1410 km distance from the Earth, which were launched between 1998 and 2000. The satellites were distributed in 8 different orbital planes with 6 equally spaced satellites per plane. Satellites complete an orbit in a bit less than 2 hours, and they use an antenna array for illuminating user terminals with a total of 16 simultaneous beams. The transfer between beams within a satellite and between satellites is carried out in a smooth way in order to keep unbroken the communication line and avoid signal outages [5].

Since the nominal lifespan of the first-generation satellites was about 15 years, a second-generation constellation was deployed between 2010 and 2013. While originally planned to consist of 32 satellites, only 24 were ultimately deployed, which are the ones currently operating. A third-generation constellation is currently under construction and planned to be launched by 2025.

B. Globalstar satellite-to-user forward links

The Globalstar satellite-to-user links operate in the S-band within the frequency range from 2483.5 to 2500 MHz, thus using a bandwidth of 16.5 MHz. Each of the 16 beams is uses this bandwidth of 16.5 MHz, which is in turn divided into 13 frequency division multiplexing (FDM) slots of 1.23 MHz bandwidth each, also referred to as *subbeams*.

Within each subbeam, an overlay of up to 128 synchronous data channels is simultaneously transmitted using a Walsh code that is subsequently spread using an in-phase and a quadrature inner spreading code sequence for code-division multiple access (CDMA). In this way, Walsh codes are used for data separation while inner spreading codes are used for emitting source separation. An unmodulated (i.e. all-zeros) pilot sequence is always transmitted in the first data channel, which is used by user terminals to search and detect the satellite to be locked to.

Inner spreading code sequences have a length of 1024 chips and a chip rate of 1.2288 MHz, therefore leading to 24 inner code repetitions within a 20 ms time period. This is contrast with the 1023 long spreading code sequences used in GPS L1 C/A, which are repeated 20 times in a 20 ms time period. This makes the Globalstar spreading code period slightly shorter than its GPS L1 C/A counterpart, with the former having a duration of $20/24 = 0.833$ ms while the latter of 1 ms. A different pair of inner spreading codes is used for each Globalstar orbital plane, meaning that all satellites within the same orbital plane do share the same pair of inner spreading codes. Within each satellite, unique offsets of the inner spreading code are used to identify adjacent beams.

Finally, each inner spreading code sequence is amplitude modulated with the chip of an overlay or outer code, which runs at a rate equal to $24/(20 \cdot 10^{-3}) = 1.2$ kcps. This outer code is used to improve the spectral properties of the transmitted signal and to increase the ambiguity range for satellite diversity purposes Additionally, unique offsets of the outer code are used to identify each satellite beam.

Based on the high-level description of the Globalstar signal, one can see that the acquisition procedure is facilitated by the fact that one of the synchronous data channels is composed of an all-zeros sequence. When this channel is modulated with the inner spreading code sequence, the same spreading code sequence is obtained, which can then easily be detected and tracked. It is true that the overlay code is still be present, but it has the same effect, and it can be handled in a similar way, as the secondary[1] code already present in some GNSS signals such as Galileo E1-C or GPS L5-Q.

C. Globalstar equivalent received signal model

The Globalstar signal is composed at its core by a pair of two different inner or primary spreading codes, one spreading the in-phase component and the other one the quadrature component. The optimal approach for processing such signal would consist on the joint acquisition and tracking of both spreading codes. However, and for the sake of simplicity, we will focus herein on the processing of one of such codes, thus assuming that we are interested in either the in-phase or the quadrature component only.

In this way, the discrete-time baseband equivalent signal of the Globalstar received pilot signal can be expressed as,

$$\begin{aligned} r(n) &= \sqrt{P_r} \sum_{i=-\infty}^{\infty} \sum_{m=0}^{N_{\mathrm{c}_2}-1} \sum_{k=0}^{N_{\mathrm{c}_1}-1} c_2(m) c_1(k) \\ &\quad \cdot p(n - kN_{\mathrm{sc}_1} - mN_{\mathrm{sc}_1}N_{\mathrm{c}_1} - iN_{\mathrm{sc}_1}N_{\mathrm{c}_1}N_{\mathrm{c}_2}) + w(n) \end{aligned} \tag{1}$$

where P_r is the received power, $c_1(k)$ is the primary spreading code sequence with length N_{c_1} chips and N_{sc_1} samples per chip, $c_2(m)$ is the secondary spreading code sequence with length N_{c_2} chips, $p(n)$ is a square-root raised cosine pulse with 0.2 roll-off factor and finally $w(n)$ is zero-mean complex Gaussian noise with power σ_w^2.

Neither the primary nor the secondary spreading code sequences are publicly available in the literature, which makes not possible to process Globalstar signals in a straightforward manner. The approach followed by this paper is to concentrate on generating potential sequences for the primary spreading code, while disregarding the secondary code. Actually, the latter can be treated as a sequence of unknown data-modulating symbols, and then proceed similarly to what is done in conventional GNSS receivers when processing data-modulated signal components (e.g. GPS L1 C/A).

[1]For the sake of clarity, inner spreading code sequences will often be referred herein as *primary* spreading code sequences, and overlay or outer code sequences as *secondary* code sequences.

Fig. 1: Processing gain as a function of the position of the extra bit of the Globalstar E-PN sequences.

III. Generation of Globalstar Spreading Codes

According to [6], the overlay PN sequence has been selected as the first couple of Extended PN (E-PN) sequences generated by the polynomials 2273 and 2213 in octal notation. While extending pseudo-random sequences is a process also implemented in IS-95, the cellular wireless system whose physical layer served as the starting point for Globalstar, no specific details are provided in [6] on how such E-PN sequences are implemented for Globalstar. In this work we use the 10-bit LFSR resulting from the 2213 polynomial referred to [6], we generate a set of tentative maximal length sequences, and finally we find the right position where to add the missing extra bit. The criterion for doing so is based on maximizing the height of the resulting correlation between the received Globalstar signal and the tentative local replica being tested. There are additional factors, though, that need to be accounted for in order to maximize the peak, such as the 10-bit sequence orientation, direct or reverse. Results are briefly summarized in Fig. 1 for a couple of tentative sequences.

We identified three pairs of 10-bit LFSR sequences that provide a high-enough correlation peak when used to process recorded live Globalstar signals. Each pair is common to all satellites within the same orbital plane, which is in agreement with the definition of the Globalstar system.

Sequence Pair I	Sequence Pair II	Sequence Pair III
M073	M092	M082
M090	M089	M080
M083	M086	M077
M081	M085	M074
M076	M94	M097
M093	M078	M096
M088		M095
		M091
		M079

TABLE I: List of satellites that are found to be using the pairs of E-PN sequences being tested in this work.

The couple of maximal length LFRS for **Sequence Pair I** are generated by polynomials **32D** and **3A3** respectively. Similarly, maximal length LFSR **Sequence Pair II** are generated by polynomials **213** and **298** respectively. And finally, maximal length LFSR for **Sequence Pair III** are generated by

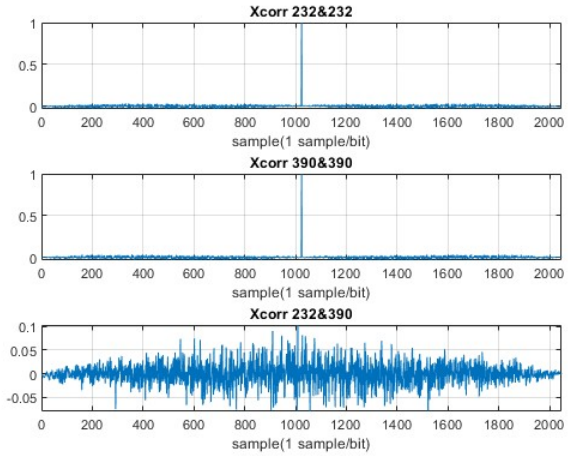

Fig. 2: (Subplot311) 1024 bits sequence 232 autocorrelation, (Subplot312) 1024 bits sequence [390] autocorrelation, (Subplot313) 1024 bits sequences [232/290] crosscorrelation.

polynomials **232** and **390** respectively. In each case, a zero is padded at the beginning of the 1023 sequence to get a 1024 bit sequence.

Out of all possible 10-bit LFSRs sequences polynomials, there are only 64 polynomials with maximal sequences, given by table II.

204	20D	213	216	232	237	240	245	262
26B	273	279	27F	286	28C	291	298	29E
2A1	2AB	2B5	2C2	2C7	2CB	2D0	2E3	2F2
2FB	2FD	309	30A	312	31B	321	327	32D
33C	33F	344	35A	360	369	36F	37E	38B
38E	390	39C	3A3	3A6	3AA	3AC	3B1	3BE
3C6	3C9	3D8	3ED	3F9	3FC			

TABLE II: List of all the 10bit-polynomials for maximal length LFSRs sequences.

If an extra zero is appended to the 1023-bit sequences generated by the 10-bit polynomials 232 and 390, forming a 1024-bit sequence, and the sequence is flipped, the resulting 1024-bit sequences are no longer maximal-length. However, they retain specific autocorrelation and cross-correlation properties, as illustrated in Figure 2.

IV. Simulation Results

The goal of this section is to assess the goodness of the E-PN primary spreading code sequences identified in Section III. To do so, a set of recorded live samples from Globalstar satellites is used, corresponding to subbeam #9 centered at 2494.23 MHz and sampled at a rate of 12.5 MHz.

A. Experiment #1: Normalized correlation peak

Figure 3 shows a set of overimposed correlation peaks of the received Globalstar, where it can be seen the smooth shape and part of the secondary lobes of the square-root raised cosine pulse used by Globalstar signals. The upper subplot displays the normalized correlation peaks across various time intervals, where some asymmetry is observed on the right hand side, where no secondary lobe is observed. This could presumably

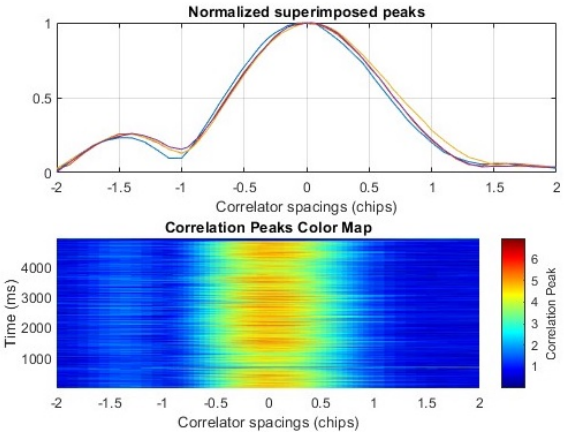

Fig. 3: Normalized correlation peak of the Globalstar signal under test.

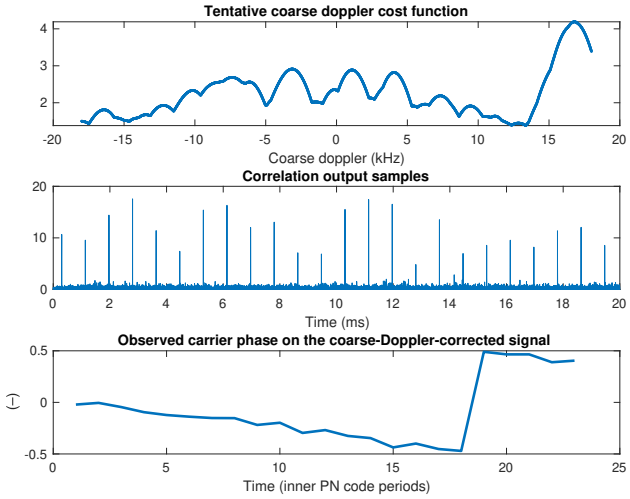

Fig. 4: Correlation peaks obtained in open-loop (i.e. snapshot mode).

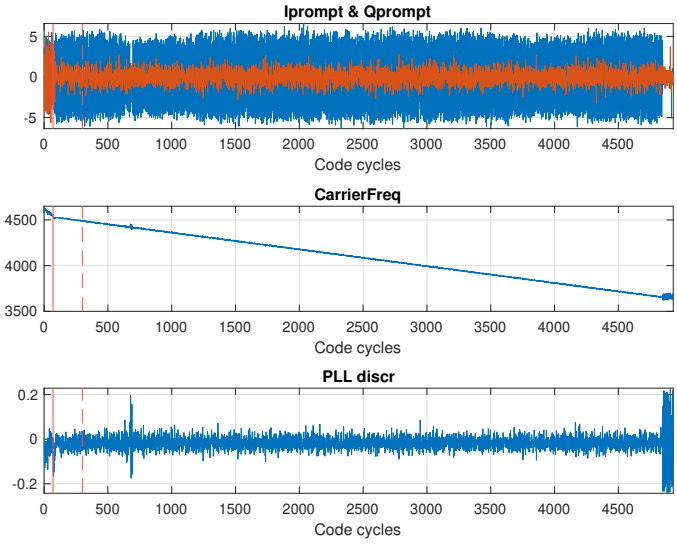

Fig. 5: Tracking results.

be due some residual far-distant multipath contribution affecting in a destructive manner on the right hand side secondary lobe of the correlation peak. The lower subplot illustrates the evolution of the correlation peak shape over time, once both the carrier and code tracking loops have achieved lock. The amplitude of the peaks is found to decrease at some time instants, and effect that is also observed on the input samples, and probably due to instabilities on the hardware devices being used for the recording.

B. Experiment #2: Open-loop prompt correlator values

The results in Fig. 4 correspond to the output provided by the open-loop or snapshot processing of Globalstar samples for subbeam #9 of satellite Globalstar M073. The top subplot shows the value of the cost function for determining the coarse Doppler, which essentially consists in a grid search where the received samples are correlated with a local replica using tentative values of the Doppler frequency. As can be seen, the most likely coarse Doppler is ~ 18 kHz, but some other tentative Dopplers do also score relatively high. This is due to the mismatch between the actual primary code sequence and the one determined following the procedure in Section III. Nevertheless, and despite of such mismatch, the middle plot shows that very-well defined correlation peaks are obtained when correlating the coarse Doppler compensated received signal with such partially-known sequence. Finally, the lower plot shows the phase of such correlation peaks, where a well-defined trend is observed, in line with a phase still being affected by a small residual Doppler after coarse Doppler compensation. The results in Fig. 4 confirm that the primary spreading code sequences described in Section III are able to achieve a successful acquisition and provide prompt correlation values to be used later on for tracking purposes.

C. Experiment #3: Closed-loop carrier tracking

The results shown in Fig. 5 correspond to the output provided by the closed-loop tracking stage of a GNSS software receiver that was modified to make it compatible with Globalstar signals. As can be seen in the top subplot, the receiver is able to keep track of the in-phase component, where the chips of the secondary code can be observed as binary data-modulated symbols. In the middle subplot, a rather clean estimate of the Doppler frequency can be observed, thus confirming that receiver is able to keep track of the Globalstar signal. This is further confirmed with the bottom subplot where the PLL discriminator output is shown, providing a very small value in line with the fact that the signal is being properly tracked.

V. Conclusions

Globalstar are signals are interesting for opportunistic positioning using LEO signals due to their CDMA structure, similar to the one adopted by most of the existing GNSS. This provides interesting synergies between Globalstar and GNSS receiver signal processing, and the combined use of Globalstar and GNSS for improved and robust positioning in denied or adverse working conditions. The main problem for processing Globalstar signals is that the spreading code sequences used transmitted by Globalstar satellites are not explicitly available in the existing literature. This makes difficult to process such signals without additional information. This paper has unveiled

some hints on how Globalstar spreading codes could have been generated, providing experimental results that confirm the successful acquisition and tracking of such signals. While knowledge of the Globalstar spreading code sequences is not yet complete, the results of this paper unveil a potential way forward where further analysis could be conducted.

ACKNOWLEDGMENT

The authors would like to thank the European Space Agency (ESA) for providing recorded samples of Globalstar signals, available at the Navigation Laboratory of the European Space Research and Technology Center (ESTEC), Noordwijk, The Netherlands.

REFERENCES

[1] M. Orabi, J. Khalife, and Z. M. Kassas, "Opportunistic navigation with Doppler measurements from Iridium Next and Orbcomm LEO satellites," in *2021 IEEE Aerospace Conference (50100)*. IEEE, 2021, pp. 1–9.

[2] Z. Kassas, S. Kozhaya, J. Saroufim, H. Kanj, and S. Hayek, "A look at the stars: Navigation with multi-constellation LEO satellite signals of opportunity," *InsideGNSS*, July/August 2023.

[3] M. Neinavaie, J. Khalife, and Z. M. Kassas, "Blind doppler tracking and beacon detection for opportunistic navigation with LEO satellite signals," in *IEEE Aerospace Conference*. IEEE, 2021, pp. 1–8.

[4] Y. Zhang, H. Qin, and G. Shi, "Doppler positioning based on global-star signals of opportunity," in *International Conference on Electronic Engineering and Informatics (EEI)*. IEEE, 2023, pp. 666–669.

[5] Globalstar L.P., "Description of the Globalstar system," GS-TR-94-001, Revision E, December 7 2000.

[6] R. De Gaudenzi, "Payload nonlinearity impact on the Globalstar forward link multiplex: I. Physical layer analysis," *IEEE Trans. Veh. Technol.*, vol. 48, no. 3, pp. 960–976, 1999.